

# Determination of Binding Constants by Flow Injection Gradient Technique

Chieu D. Tran,\* Mauricio S. Baptista, and Takuya Tomooka

Department of Chemistry, Marquette University, P.O. Box 1881, Milwaukee, Wisconsin 53201

Received May 19, 1998. In Final Form: September 17, 1998

A new method is based on the flow injection gradient equipped with an acousto-optic tunable filter (AOTF) detector has been developed for the determination of binding constants of substrates with cyclodextrins or micelles. The concentration gradient produced by this method eliminates the need to prepare series of mixtures in which the concentrations of one of the reactants are varied. The fast scanning ability of the AOTF enables the detector to record the whole absorption spectrum of the mixture as it flows through the flow cell. Binding constants can be rapidly determined. The effectiveness of the method was evaluated by determining binding constants of inclusion complex formation between  $\beta$ -cyclodextrin ( $\beta$ -CD) and phenolphthalein and of the incorporation of organic molecules (e.g., *p*-toluenesulfonic acid (PTS) and benzophenone (BP)) into micelles (CTAB) under steady state condition (no flow) and compared with values determined under the flow injection gradient. The method is particularly effective for charged substrates, e.g., the binding constants obtained between PTS and CTAB and between phenolphthalein and  $\beta$ -CD. Neutral substrate, BP, gives relatively poor accuracy and reproducibility, and these may be due to the adsorption of the substrate onto the flow device.

## Introduction

Complex formations through noncovalent interactions are known to play an essential role in processes such as enzymatic reactions, drug delivery, and chiral separations. Because of the importance, they have been a subject of intense studies.<sup>1,2</sup> Techniques such as spectrophotometry,<sup>3</sup> fluorometry,<sup>4</sup> calorimetric titrimetry,<sup>5</sup> circular dichroism,<sup>6</sup> NMR,<sup>7</sup> HPLC,<sup>8</sup> and potentiometry,<sup>9</sup> have been used to measure binding constants. Usually, in these methods, it is required to measure a series of mixtures in which the concentration of one of reactants is varied. As such, these methods are time consuming and prone to large experimental error.<sup>1</sup>

Flow injection analysis (FIA) has been used extensively in process analyses because of its simplicity, rapidity, economy, and wide applicability. Among different modes of operation, the flow injection gradient (FIG) is perhaps the most widely used technique. The gradient can be generated by using different devices (e.g., a mixing chamber) placed in-line with the sampling valve and flow cell. The concentration profiles generated are reproducible and can be used for study where a smooth time variable concentration profile is required. As a consequence, the concentration gradient generated not only can replace the manual preparation and the measurement of several solutions with different concentrations of the reactants but also can increase the velocity, precision, and accuracy of the determinations.<sup>10</sup> In fact, the FIG technique has

been successfully used for accurate and automated determination of formation constants of various chemical systems<sup>11–13</sup> and for the characterization of a variety of chemical systems including acidity constants<sup>14</sup> and proton–ligand equilibria. The FIG technique can also be used to determine binding constants between fluorescent probes and drugs to proteins.<sup>15</sup> It is possible to use the FIG technique to generate concentration profiles for systems such as the inclusion complex formation between  $\beta$ -CD and phenolphthalein, and the incorporation of organic molecules (*p*-toluenesulfonic acid and benzophenone) into aqueous micelles. The profiles obtained can then be used to determine the binding constants. This type of study can only be performed if the detection technique used in the FIG is capable of rapidly recording entire spectra of samples as they are flowing through the detector. A spectrometer equipped with a diode array can serve as a detector for such a study. However, this type of multi-channel detector suffers from relatively low sensitivity and is rather expensive. Fortunately, a sensitive, inexpensive detector capable of rapidly recording an absorption spectrum of a flowing sample can be constructed with the recently developed acousto-optic tunable filter.

An acousto-optic tunable filter (AOTF) is an all solid state, electronic monochromator, which is based on the diffraction of light by an acoustic wave in an anisotropic crystal.<sup>16–22</sup> The filter can diffract incident white light at

(1) Connors, K. A. *Binding Constants—The Measurement of Molecular Complex Stability*; Wiley: New York, 1987.  
(2) Cram, D. J.; Cram, J. M. *Container molecules and their guests*; Royal Society of Chemistry: Great Britain, 1994.  
(3) Pendergast, D. D.; Connors, K. A. *J. Pharm. Sci.* **1984**, *73*, 1779.  
(4) Edelman, G. M.; McClure, W. O. *Acc. Chem. Res.* **1968**, *1*, 65.  
(5) Cromwell, W.; Bystroem, K.; Eftink, M. R. *J. Phys. Chem.* **1985**, *89*, 326.  
(6) (a) Han, S. M.; Purdie, N. *Anal. Chem.* **1984**, *56*, 2822. (b) Han, S. M.; Purdie, N. *Anal. Chem.* **1984**, *56*, 2825.  
(7) Carper, W. R.; Buess, C. M.; Hipp, G. R. *J. Phys. Chem.* **1970**, *74*, 4229.  
(8) Arunyanart, M.; Love, L. J. *Anal. Chem.* **1984**, *56*, 1557.  
(9) Takisawa, N.; Hall, D.; Wyn-Jones, E.; Brown, P. *J. Chem. Soc., Faraday Trans. 1* **1988**, *84*, 3059.

(10) Georgiou, M. E.; Georgiou, C. A.; Koupparis, M. A. *Anal. Chem.* **1995**, *67*, 114.  
(11) Betteridge, D.; Fields, B. *Anal. Chim. Acta* **1981**, *132*, 139.  
(12) Turner, D. R.; Santos, M. C.; Coutinho, P.; Goncaves, M. L.; Knox, S. *Anal. Chim. Acta* **1992**, *258*, 259.  
(13) Růžička, J.; Hansen, E. H. *Flow Injection Analysis*, 2nd ed.; Wiley: New York, 1988.  
(14) Vacárcel, M.; Luque de Castro, M. D. *Flow-Injection Analysis, Principals and Applications*; Ellis Horwood Limited: Chichester, U.K., 1987.  
(15) Miller, J. N.; Abdullahi, G. L.; Sturley, H. N.; Gossain, V.; McCluskey, P. L. *Anal. Chim. Acta* **1986**, *179*, 81.  
(16) Tran, C. D. *Anal. Chem.* **1992**, *64*, 971A.  
(17) Tran, C. D.; Bartelt, M. *Rev. Sci. Instrum.* **1992**, *63*, 2939.  
(18) Tran, C. D.; Furlan, R. *J. Anal. Chem.* **1992**, *64*, 2775.  
(19) Tran, C. D.; Furlan, R. *J. Anal. Chem.* **1993**, *65*, 1675.  
(20) Tran, C. D.; Lu, J. *Anal. Chim. Acta* **1995**, *314*, 57.

a specific wavelength when a specific radio frequency (RF) is applied into it. The wavelength of the diffracted light can be scanned over a large optical region by simply changing the frequency of the applied RF. The compact, all-solid-state AOTF is rugged, has a wide acceptance angle and tuning range (from UV through visible to IR), high throughput, and high-speed random wavelength access. Additionally, the tunable filter has been demonstrated to have high spectral resolution ( $0.82 \text{ \AA}$  at  $253.4 \text{ nm}$ )<sup>20</sup> and fast scanning ability (microseconds).<sup>18–20</sup> These features make it possible to use the AOTF to develop novel instruments that are not possible otherwise. For instance, we have recently demonstrated that a spectrophotometer based on AOTF is capable of sensitively and rapidly recording the entire absorption spectra of compounds as they elute from an HPLC column<sup>20</sup> or in FIA.<sup>22</sup> Prior work clearly indicates that it is possible to use the AOTF-based UV–visible absorption detector as a sensitive and fast scanning detector for FIG. The aim of this study is to synergistically use the FIG and the AOTF based detector to develop a novel method for the accurate and rapid determination of binding constants of inclusion complex formation between  $\beta$ -CD and phenolphthalein, and the incorporation of organic molecules (e.g., *p*-toluene sulfonic acid and benzophenone) into aqueous micelles. The effectiveness of the FIG-AOTF-based detector will be evaluated by comparing the results obtained using a conventional spectrophotometer to study nonflowing systems to those obtained using the FIG-AOTF-based detector (for flowing systems in the FIG). Advantages as well as limitations of the FIG-AOTF-based detector system will be discussed in this paper.

### Experimental Section

**Materials.** Deionized water was distilled in an all-glass apparatus. Sodium dodecyl sulfate (SDS, electrophoretic grade) and hexadecyltrimethylammonium bromide (CTAB, electrophoretic grade) were obtained from Kodak. Polyoxyethylene-(23) dodecyl ether (Brij-35),  $\beta$ -cyclodextrin, and *p*-toluenesulfonic acid monohydrate (PTS) were purchased from Aldrich. Benzophenone (BP) was purchased from Fisher Scientific. Phenolphthalein was obtained from Merck. Buffer solutions were prepared by dissolving an appropriate amount of salt ( $\text{NaH}_2\text{PO}_4$  or  $\text{Na}_2\text{CO}_3$ ) and adjusting the pH with either HCl or NaOH.

**Instrumentation.** The instrument utilized, i.e., UV–vis flow injection gradient (UV–vis-FIG) was designed to generate concentration gradients and to measure absorption spectra in the UV–vis region. The instrument (Figure 1) consisted of a peristaltic pump (Pump) (Gilson Minipuls 2) to deliver the solvent and the sample through the single line manifold that contained a sample injector (I), a homemade Teflon mixing chamber (MC) and a flow cell (FC). Two sample injectors were used: for the first set of experiments (section 1) the injector was made of Teflon with a sample volume of  $108 \mu\text{L}$ . A HPLC injector (Rheodyne, Model 7125) was used for the second set of experiments. The flow cell used in the section 1 experiments was made of Teflon with a 1.7-cm path length and 3-mm diameter. The Teflon FC used in section 2 had 0.75-cm path length and 4-mm diameter. Either a home-built UV–vis-AOTF spectrophotometer (Figure 1) or the Perkin-Elmer spectrophotometer (Model 320) was used as a detector. A 250-W halogen tungsten lamp (Osram HLX 64655) provided light in the visible, and a 150-W xenon arc lamp (Oriel Corp) was for UV light in the AOTF-based spectrophotometer. The collimated incident white light from one of these two light sources was dispersed by monochromatic light and spectrally scanned by means of an AOTF. Depending on the spectrum region, one of two AOTF's was used. A noncollinear AOTF (Brimrose, Baltimore, Model TEAF-X40-70H) was used

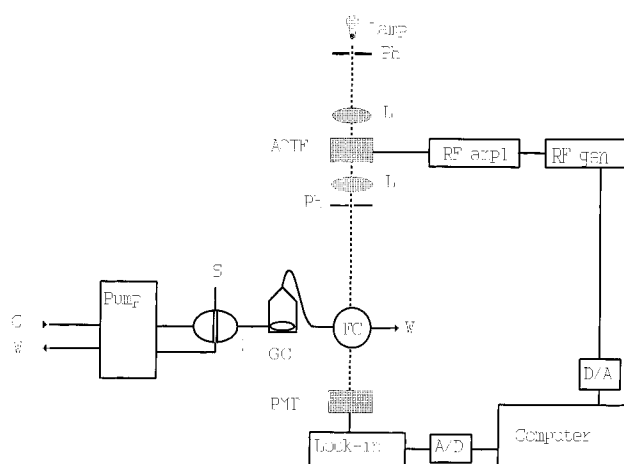


**Figure 1.** Schematic diagram of the UV–vis-FIG instrument: W, waste; C, carrier; Pump, peristaltic pump; S, sample; I, injector; MC, mixing chamber; FC, flow cell; Ph, pinhole; Po, polarizer; L, lens.

for the visible region (from 400 to 650 nm). For the 250–650 nm region, a collinear AOTF (International Scientific Products Co., New York, Model Q1101), was used. An RF synthesizer (Wavetek, Inc., Model 5131-01-1026) provided the RF signal. The RF signal was amplitude-modulated at 50 kHz by a home-built modulator and amplified by a RF power amplifier (ENI, Model 411LA) before being applied to the AOTF. The light diffracted from the AOTF was focused into the flow cell by a lens. The intensity of the transmitted light was detected by a photomultiplier tube (PMT) (Cary Applied Physics, Co., Model RCA IP28). A slit was placed in front of the PMT to reduce the background noise. The output signal from the detector, which was AM modulated at 50 kHz, was connected to a lock-in amplifier (Stanford Research Systems Model SR 510) for demodulation and amplification. The signal from the lock-in amplifier was then connected to a microcomputer (Gateway 2000 DX2 50 MHz) through a 16 bit A/D interface board (National Instruments Model AT MIO 16X). A software written in C++ language was used to control the frequency and the power and to scan the applied RF signal. The same software also facilitated the data acquisition and analysis (e.g., to calculate the absorption spectra) and saved the data in ASCII format for the subsequent data analysis using other software packages (e.g., Gram-386 and Slide-Write). An optical switch was used to synchronize the introduction of the sample solutions into the FIG manifold and the start of the data acquisition.

The absorption spectra were measured in either a Shimadzu UV–vis (UV-1201) or a Hewlett-Packard diode array (8452A) spectrophotometer.

### Results and Discussion

To clarify the presentation of the results and to facilitate discussion, this part of the paper will be subdivided into two sections. The first section describes the complex formation between  $\beta$ -CD and phenolphthalein, and the second section is for the complexes between micelles and two different substrates, i.e., *p*-toluenesulfonic acid and benzophenone.

**I. Binding Constants of  $\beta$ -CD and Phenolphthalein.** The determination of the  $\beta$ -CD–phenolphthalein host–guest association constant will be presented to demonstrate the fundamentals and advantages of the FIG method. Its application to more complex systems, i.e., determination of binding constants in micellar systems, will be determined in the second section.

To calculate the binding constant of a complexation reaction using the FIG technique, it is necessary to generate a concentration gradient of ligand (e.g.,  $\beta$ -CD) as a function of time. The concentration gradient will

(21) Politi, M. J.; Tran, C. D.; Gao, G. H. *J. Phys. Chem.* **1995**, *99*, 14137.

(22) Pasquini, C.; Lu, J.; Tran, C. D.; Smirnov, S. *Anal. Chim. Acta* **1996**, *319*, 315.

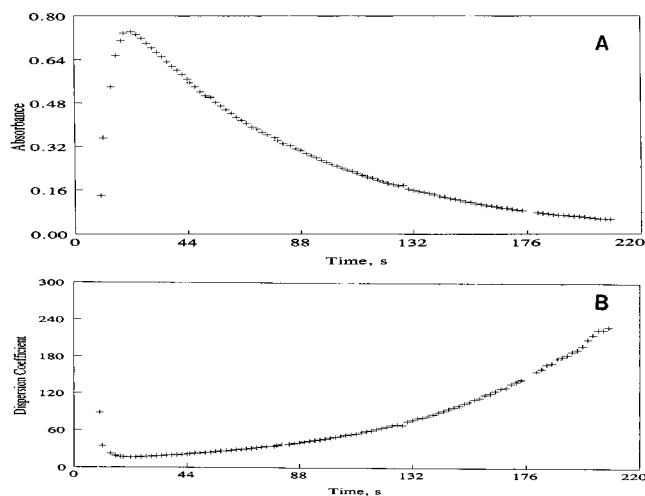


**Figure 2.** (a) Absorbance at 550 nm measured as a function of time after injecting  $2.75 \times 10^{-5}$  M phenolphthalein solution; [carbonate buffer] = 0.02 M, pH = 10.5, flow rate = 3 mL/min. (b) Dispersion coefficient (eq 1) as a function of time measured with a  $2.75 \times 10^{-5}$  M phenolphthalein solution; [carbonate buffer] = 0.02 M, pH = 10.5, flow rate = 3 mL/min.

then be calibrated for subsequent use in the determination of the binding constants. The calibration is performed with a compound whose molar extinction coefficient is known (i.e., phenolphthalein). The absorbance at 550 nm measured as a function of time, after injecting 108  $\mu$ L of  $2.75 \times 10^{-5}$  M phenolphthalein solution into the FIG device is shown in Figure 2a. The absorption reached a maximum 22 s after the injection, followed by a slow decrease. This absorption profile can be explained by the concentration profile of phenolphthalein that was generated in the mixing chamber and monitored in the flow cell. There was a fast mixing of the phenolphthalein with the carrier solvent after the sample (phenolphthalein) was injected into the mixing chamber. As a consequence, the concentration of the sample started to increase inside the flow cell. The absorption reached its maximum value when the mixing is completed. Thereafter, the only remaining effect was the dilution of the phenolphthalein inside the MC by the solvent that has been continuously pumped into the chamber. This dilution profile generates a large array of different concentration segments, which can be used to calculate any system parameter that is dependent on the concentration of the injected species (e.g., binding constant). The absorption as a function of time (Figure 2a) can be easily converted into concentration as a function of time by using phenolphthalein's molar extinction coefficient ( $\epsilon = 2.65 \times 10^4$  M $^{-1}$  cm $^{-1}$  at 550 nm).<sup>10,23</sup> To facilitate the calibration of the concentration gradient, it is important to express the concentration profile independently of the injected concentration of the standard. This is because, after the gradient is calibrated, it can then be used to calculate the concentration gradient of other samples or substances. Thus, it is common to plot dispersion coefficient versus time instead of concentration versus time. The dispersion coefficient indicates the dilution of the sample at a specific time:

$$D_{\text{time}} = \frac{[\text{Ph}]_0 \epsilon}{A_{\text{time}}} \quad (1)$$

where  $[\text{Ph}]_0$  is the concentration of stock solution of

phenolphthalein,  $\epsilon$  is the phenolphthalein molar extinction coefficient, and  $A_{\text{time}}$  is the absorbance measured as a function of time. Figure 2b shows the dispersion coefficient as a function of time calculated from the results shown in Figure 2a for phenolphthalein. Note that at 22 s after the injection  $D_{\text{time}}$  reaches its minimum ( $D_{\text{time}} = 16.4$ ). This result indicates that 22 s after the injection the sample was diluted 16.4 times. It is important to emphasize that  $D_{\text{time}}$  is known to be independent of the type and concentration of the molecule used in the calibration (as long as the solution viscosity remains the same). Furthermore, it is fairly reproducible in repetitive experiments.<sup>10,13,14</sup> If the flow rate is kept constant, the dispersion coefficient plot can be used to calculate the concentration of any compound injected into the flow injection device at any time.

To calculate the  $\beta$ -CD-phenolphthalein binding constant, a solution (pH = 10.5) with 0.01 M of  $\beta$ -CD and  $3.20 \times 10^{-5}$  M of phenolphthalein was injected into the flow carrier, which also contains  $3.20 \times 10^{-5}$  M phenolphthalein. The absorbance (at 550 nm) versus time profile is shown in Figure 3. When the  $\beta$ -CD concentration reached its maximum (22 s after the injection), the measured absorbance was at a minimum. The absorption decreased when phenolphthalein bound to  $\beta$ -CD and became completely transparent ( $\epsilon$  of phenolphthalein/ $\beta$ -CD complex at 550 nm is zero).<sup>10,23a,23b</sup> The mechanisms for the complex formation, in relation to the change in the absorbance of phenolphthalein, are currently not well understood.<sup>23</sup> It seems that the phenolphthalein molecule interacts with at least three sites of the  $\beta$ -CD's ring. These interactions promote major changes in the electronic structure of phenolphthalein which, in turn, induces the transparency in the visible region around 550 nm.<sup>23a,b</sup> It should be realized that the minimum the absorbance reached 22 min after the injection (Figure 3) is not zero because not all phenolphthalein molecules are bound to  $\beta$ -CD, and the  $\epsilon$  for free phenolphthalein is not zero.

With the dilution of the  $\beta$ -CD, there is an increase in the solution absorption. By use of the dispersion coefficient graph (Figure 2b), the time scale of Figure 4 can be converted into a  $\beta$ -CD concentration scale, and the resulting plot becomes a characteristic binding isotherm. To obtain a numerical value for the binding constant, the experimental data must be fitted to a linear binding isotherm. The linear procedure facilitates not only the visualization of the quality of the fit between the experimental points and the theoretical model but also the estimation of the error involved in the calculation of the model parameters.<sup>1</sup>

The complexation between the ligand molecule ( $\beta$ -CD, denotes as L) and the substrate molecule (phenolphthalein, denotes as S) can be expressed by



where S-L represents the inclusion complex between  $\beta$ -cyclodextrin and phenolphthalein. The binding equilibrium constant ( $K_B$ ) is

$$K_B = \frac{[\text{S-L}]}{[\text{S}][\text{L}]} \quad (3)$$

The mass balance equations for the equilibrium are

$$[\text{S}]_{\text{total}} = [\text{S}]_{\text{free}} + [\text{S-L}] \quad (4)$$

$$[\text{L}]_{\text{total}} = [\text{L}]_{\text{free}} + [\text{S-L}] \quad (5)$$

(23) (a) Buvári, Á.; Barcza, L.; Kajtár, M. *J. Chem. Soc., Perkin Trans. 2* **1988**, 1687. (b) Taguchi, K. *J. Am. Chem. Soc.* **1986**, *108*, 2705.

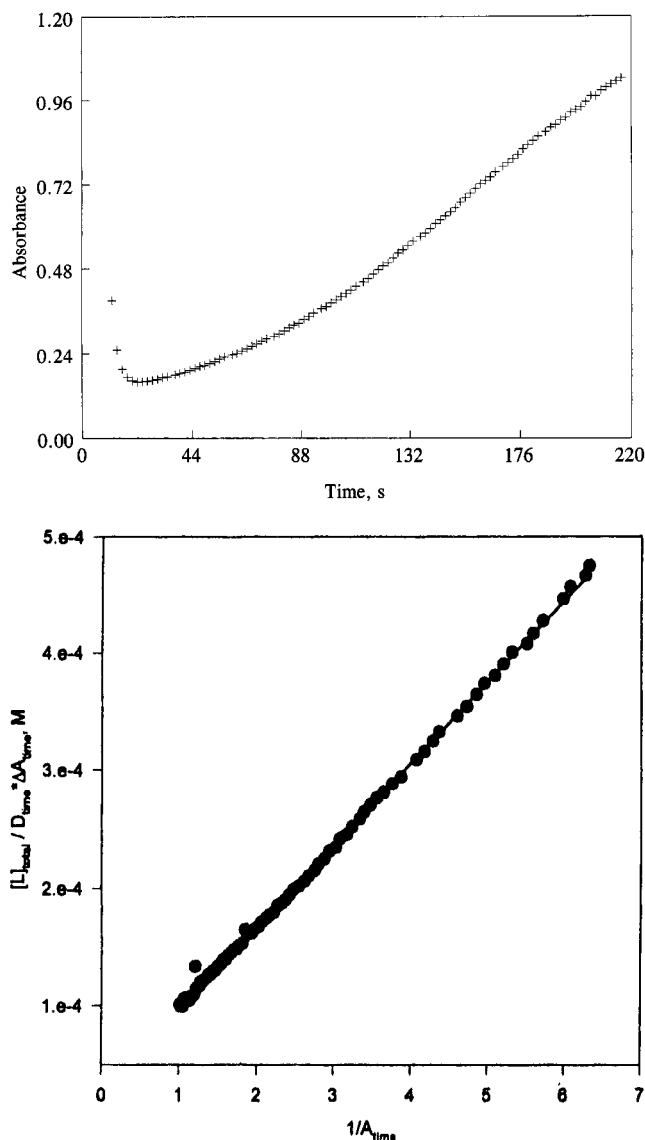


**Figure 3.** (Top) absorption as a function of time after injecting a solution containing 0.01 M  $\beta$ -cyclodextrin and  $3.2 \times 10^{-5}$  M phenolphthalein into the flow carrier ([phenolphthalein] =  $3.2 \times 10^{-5}$  M), [carbonate buffer] = 0.02 M, and pH = 10.5, flow rate = 3 mL/min. (Bottom) double-reciprocal plot according to eq 7 (i.e., plot of  $(L_{\text{total}}/D_{\text{time}}) (\Delta A)$  as a function  $(1/\text{Abs})$  ([phenolphthalein] =  $3.2 \times 10^{-5}$  M), [carbonate buffer] = 0.02 M, and pH = 10.5).

where subscript "free" means that the species is not complexed. Since neither the  $\beta$ -CD nor the S-L complex absorb at 550 nm, the absorption change observed with the increase in the  $\beta$ -CD concentration (as a function of time in Figure 3) can be expressed by

$$\Delta A_{\text{time}} = b\epsilon[S-L]_{\text{time}} \quad (6)$$

Combining eqs 1–6, and considering that the free ligand concentration is much larger than the concentration of complex ( $[L]_{\text{free}} \gg [S-L]$ ), yields

$$-\frac{[L]_{\text{(total)}}}{\Delta A_{\text{(time)}} D_{\text{time}}} = \frac{1}{A_{\text{time}} K_B} + \frac{1}{\epsilon b} \quad (7)$$

where  $b$  is the cell path length.

Equation 7 is a linear expression of the binding isotherm. It indicates that the plot of  $[L]_{\text{total}}/(\Delta A D_{\text{time}})$  as a function

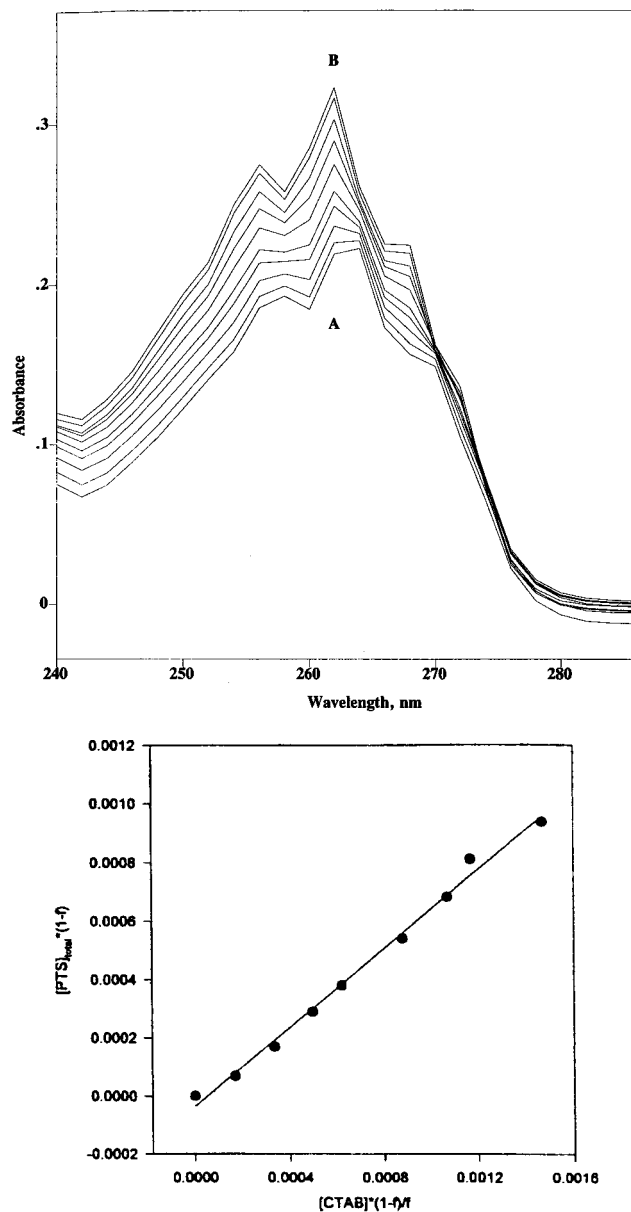


**Figure 4.** (Top) absorption spectra of  $1.0 \times 10^{-3}$  M PTS solutions in water with different concentrations of CTAB. From B to A [CTAB] = 0.00, 0.97, 2.73, 5.00, 7.50, 10.15, 12.20, 16.60, 23.30,  $30.00 \times 10^{-4}$  M. (Bottom) CTAB-PTS complexation reaction in water. Plot of  $[PTS]_{\text{total}}(1-f)$  as a function of  $[CTAB]^{(1-f)}/f$  according to eq 14.

of  $1/A_{\text{time}}$  should yield a straight line with a slope of  $1/K_B$  and an intercept equal to  $1/\epsilon b$ .

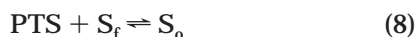
The bottom panel of Figure 3 shows the experimental data of Figure 3 treated according to eq 7. It is evident that the experimental points fit well to eq 7. The binding constant,  $(1/\text{slope})$ , was calculated to be  $(1.44 \pm 0.01) \times 10^4 \text{ M}^{-1}$ . This value is in agreement with those reported in the literature, which are in the range from  $0.2$  to  $3.5 \times 10^4 \text{ M}^{-1}$ , depending on the specific electrolyte medium employed and its concentration.<sup>24</sup> The value obtained in this work is slightly different from the values of  $(2.2-2.3) \times 10^4 \text{ M}^{-1}$  determined by Georgiou et al.<sup>10</sup> This is hardly surprising considering the differences in the experimental conditions of the two experiments, namely no buffered solution was used in the present work whereas in the ref 10, 0.020 M carbonate-buffered solutions at pH 10.5 were used.

(24) Buvári, I.; Barcza, L. *Inorg. Chim. Acta* **1979**, *33*, L179.

In summary, it has been successfully demonstrated that with only a few injections into the FIG instrumentation, it is possible to obtain the binding constant of the inclusion complexes between  $\beta$ -CD and phenolphthalein. This methodology is not restricted to this specific measurement but is rather applicable to any type of complexation process that can induce changes in the spectral properties of the complexant agents. In the next section this technique will be used for the determination of binding constants of different substrates with aqueous micelles.

**II. Binding Constants for Interaction of *p*-Toluenesulfonic Acid and Benzophenone with CTAB Micelles.** Shown in Figure 4 are the absorption spectra of *p*-toluenesulfonic acid (PTS) solutions containing different concentrations of CTAB. As illustrated, concomitant with the increase in the concentration of CTAB is a decrease in the absorbance over the entire wavelength region. This effect, which is in agreement with earlier investigations, can be explained by the incorporation of PTS into the micelle interfaces.<sup>25</sup> Since the substrate and surfactant have opposite charges, the interactions between them are expected to be strong. The strong binding with CTAB induces a change in the PTS electronic structure, which, in turn, leads to a decrease in its molar absorptivity.

Unlike the cyclodextrin binding model, we must consider a new model in which the CTAB micelles have several binding sites, with a new parameter  $N$  defined as the number of CTAB molecules per binding site. Each binding site accepts only one PTS molecule. The complexation reaction and equilibrium can be expressed by



$$K_B = \frac{[S_o]}{[S_f][\text{PTS}]_f} \quad (9)$$

where PTS is *p*-toluenesulfonic acid, S is the binding site, and the subscripts  $f$  and  $o$  represents free and occupied, respectively. The mass balance equations are

$$[\text{PTS}]_f + [S_o] = [\text{PTS}]_{\text{total}} \quad (10)$$

$$[\text{CTAB}] = N[S_o] + N[S_f] \quad (11)$$

where  $N$  is the number of CTAB molecules per binding site. The absorption change as a function of surfactant concentration will be used to calculate the fraction of bound PTS molecules ( $f$ ):

$$f = \frac{[S_o]}{[\text{PTS}]_{\text{total}}} = \frac{A - A_0}{[\text{PTS}]_{\text{total}}(\epsilon_{\text{PTS}}^{\text{MIC}} - \epsilon_{\text{PTS}}^{\text{WATER}})} \quad (12)$$

Note that  $[S_o]$ , i.e., the concentration of occupied sites, is the same as the concentration of bound PTS, because the model assumes that a binding site can accept only one PTS molecule. Equations 10–12 are substituted into eq 9 to yield the binding isotherm:

$$K_B = \frac{fN}{(1 - f)([\text{CTAB}] - fN[\text{PTS}]_{\text{total}})} \quad (13)$$

Equation 13 can be further rearranged to

$$\text{PTS}_{\text{total}}(1 - f) = -\frac{1}{K_B} + \frac{(1 - f)[\text{CTAB}]}{fN} \quad (14)$$

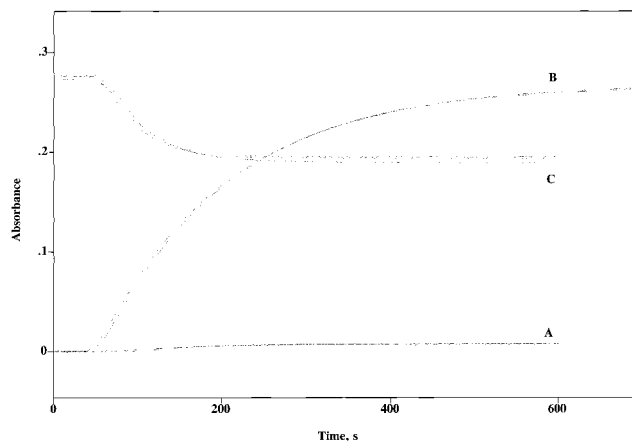


**Figure 5.** Absorbance as a function of time measured after the injection of  $3.0 \times 10^{-3}$  M CTAB solution into the water flow carrier (A),  $1.0 \times 10^{-3}$  M PTS solution into the water flow carrier (B), solution with  $3.0 \times 10^{-3}$  M CTAB and  $1.0 \times 10^{-3}$  M PTS into the flow carrier ( $1.0 \times 10^{-3}$  M PTS solution) (C). The flow rate was 1.5 mL/min,  $\lambda = 262$  nm.

**Table 1.**  $K_B$  and  $N$  for the Complexation of *p*-Toluenesulfonic Acid and Benzophenone with CTAB Micelles

$10^{-3}$ ligand (M)	flow rate (mL/min)	$10^4 K_B$ ( $M^{-1}$ )	$N$
[PTS] = 1.0	no flow	$3 \pm 1$	$1.48 \pm 0.05$
[BP] = 0.028	no flow	$3 \pm 1$	$50 \pm 2$
[PTS] = 1.0	1.5	$2.6 \pm 0.1$	$1.286 \pm 0.005$
[PTS] = 1.0	1.5	$3.4 \pm 0.2$	$1.338 \pm 0.005$
[PTS] = 1.0	1.5	$3.8 \pm 0.2$	$1.549 \pm 0.005$

Therefore, the plot of  $\text{PTS}_{\text{total}}(1 - f)$  as a function of  $[\text{CTAB}](1 - f)/f$  should yield a straight line with intercept equal to  $-1/K_B$  and with slope equals to  $1/N$ . The experimental data (absorbance at 262 nm as a function of PTS concentration) were then rearranged and plotted in accordance to eq 14 (bottom panel of Figure 4). The  $K_B$  value was calculated to be  $(3.0 \pm 1) \times 10^4 M^{-1}$  and the  $N$  value was calculated to be  $1.48 \pm 0.05$ . These values are similar to values of  $2.20 \times 10^4 M^{-1}$  and  $N = 1.3$ , which were obtained by Sepulveda using also a spectrophotometric technique without flow.<sup>25</sup>

The complexation between PTS and CTAB was then measured in the flow injection device. Shown in Figure 5 is the absorbance as a function of time measured after the injection of several solutions into the FIG device. Curves A are the absorbance as a function of time after injecting  $3.0 \times 10^{-3}$  M CTAB solutions into the flow carrier (two different injections are shown). Curves B are the absorbance as a function of time measured after injecting  $1.0 \times 10^{-3}$  M PTS solutions into the water flow carrier (two different injections are shown). Curves C are the absorbance as a function of time after the injection of solutions containing  $3.0 \times 10^{-3}$  M CTAB and  $1.0 \times 10^{-3}$  M PTS into the flow carrier ( $[\text{PTS}] = 1.0 \times 10^{-3}$  M) (the data shown are from three different injections). Using the same method described earlier, curve B was used for the calculation of the dispersion coefficient, the average of the two curves labeled as A was subtracted from each of the curves labeled as C, and curves C–A were used for the calculation of  $f$  (according to eq 12). These data were then plotted according to eq 14 to yield a straight line. The  $K_B$  and  $N$  values obtained for the three injections (curves C) are shown in Table 1. Although there is a variation in the values calculated for the three injections under the same experimental conditions, this variation is relatively small. The average of  $K_B$  and  $N$  values for the

(25) Sepulveda, L. *J. Colloid Interface Sci.* **1974**, *46*, 371.

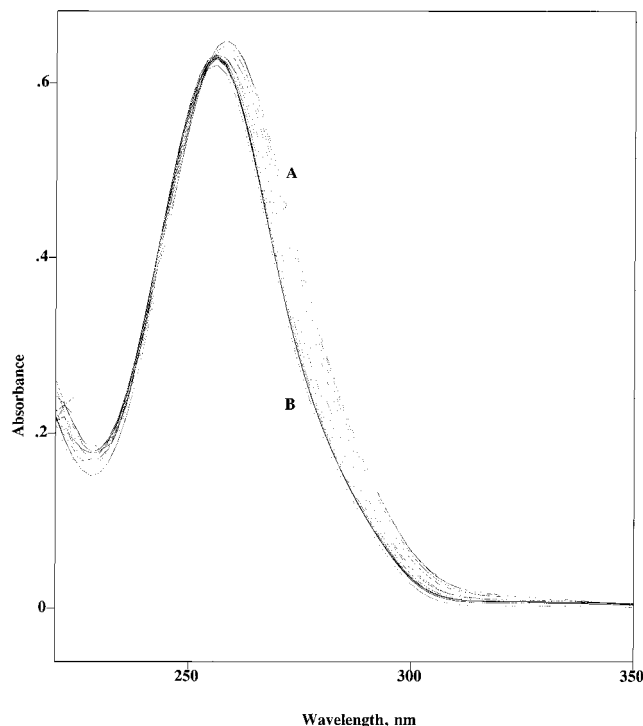


**Figure 6.** Absorption spectra of  $2.77 \times 10^{-5}$  M BP solution in water with different concentrations of CTAB. From A to B [CTAB] = 0.00, 0.99, 1.43, 2.50, 3.20, 6.25, 10.00, 11.76, 16.66, 25.00, 35.70, 43.70, 62.40, 71.80, and 100.00 mM.

three injections were found to be  $(3.3 \pm 0.6) \times 10^4 \text{ M}^{-1}$  and  $1.4 \pm 0.1$ , respectively. These values agree well with  $K_B$  and  $N$  obtained with the spectrophotometric technique without flow (Table 1). It is important to note that the  $N$  value is on the order of 1.4 for the CTAB-PTS interaction. This indicates that each interaction site consists of 1.4 CTAB molecules per one micelle. The low  $N$  value is probably due to the electrostatic interaction between CTAB and PTS, which predicts a reaction stoichiometry close to 1:1.

It is interesting to observe that in both cases where the flow injection technique worked relatively well for the determination of binding constants, i.e.,  $\beta$ -CD/phenolphthalein and CTAB/PTS complexes, the substrates used (phenolphthalein and PTS) were charged. It may be possible that the charge state or the hydrophilic/hydrophobic balance of the substrate may be an important factor to be considered when using the flow injection technique to measure binding constants. This possibility was investigated by use of another substrate, i.e., benzophenone (BP), which is not only neutral but also hydrophobic. Any possible effect should be readily observed with this substrate.

The BP spectrum also shows an absorption change when BP interacts with CTAB micelles.<sup>25</sup> The absorption spectra of BP solutions with different CTAB concentrations are shown in Figure 6. As illustrated, concomitant with the increase in the CTAB concentration is a decrease in the absorbance and a blue shift in the BP absorption maximum. The absorption difference ( $\Delta A$ ) is the difference in the absorbance at 272 nm of BP with and without CTAB.  $\Delta A$  at 272 nm as a function of CTAB concentration can then be used to calculate  $K_B$  and  $N$  for the CTAB-BP complexation according to eq 14. The calculated  $K_B$  and  $N$  values are shown in Table 1. Although the  $K_B$  value ( $K_B = 3.0 \times 10^4 \text{ M}^{-1}$ ) of the CTAB-BP complex is similar to that found for the CTAB-PTS complex, the  $N$  value for CTAB-BP is much higher than that for CTAB-PTS (50

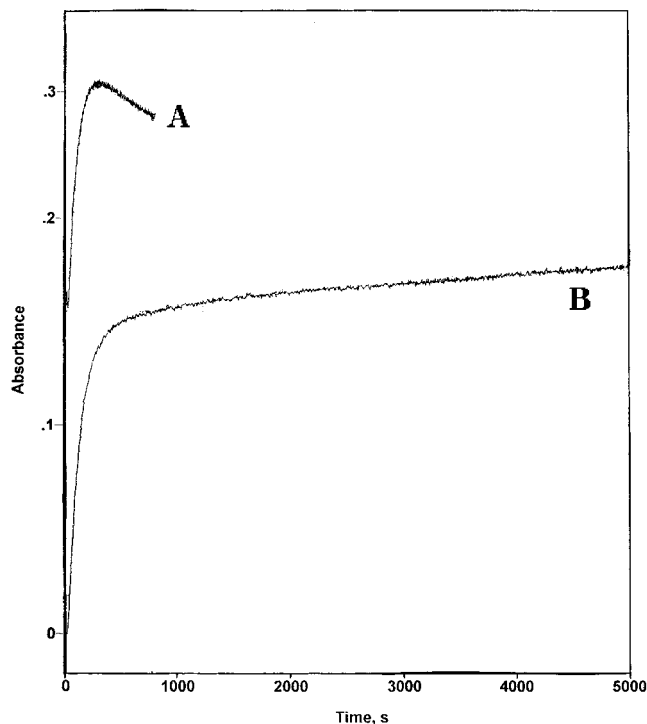


**Figure 7.** Absorption as a function of time after the injection of (A)  $7.0 \times 10^{-5}$  M BP solution into the water flow carrier, and (B) 0.04 M CTAB and  $7.0 \times 10^{-5}$  M BP solution into the flow carrier ( $7.0 \times 10^{-5}$  M BP). The Flow rate was 1.5 mL/min,  $\lambda = 272$  nm.

and 1.4, respectively). This is probably due to the difference in the interaction between these two substrates with the CTAB micelle. The CTAB-PTS interaction is mostly electrostatic, whereas the hydrophobic effect and weak van der Waals interactions are probably responsible in the case of CTAB-BP. In the case of CTAB-BP, there are an average of 50 CTAB molecules per one binding site. Considering that the aggregation number ( $n$ ) of CTAB micelles is on the order of  $(1 \times 10^2)^{27}$  ( $n$  varies from 61 to 120 depending on the method used to measure it), it is estimated that there may be about two BP molecules per one micelle.

The complexation between BP and CTAB was then measured using the flow injection device. The results obtained for this complexation reaction under flow conditions, have rather poor accuracy and reproducibility. As an example, Figure 7 shows the absorption as a function of time for two different injections. Curve A shows absorption (272 nm) as a function of time measured after the injection of  $7.0 \times 10^{-5}$  M BP solution into the water flow carrier. The absorption was measured for a long time (5000 s). Normally, the absorption as a function of time curve should level off after 900 s. However, in the case of BP the saturation was never reached, and even 5000 s after the injection, the absorbance continues to increase. It is important to emphasize that the absorption measured at 5000 s after the injection was 0.176. This value is much lower than the absorbance value of 0.290, which is expected for this solution. Therefore, it seems that the BP was lost in some part of the flow injection device. It may be possible that BP, being very hydrophobic, was adsorbed in either the Tygon, viton, or Teflon tubing of the FIG device.

(26) Fendler, J. H.; Fendler, E. J.; Infante, G. A.; Shih, P.-S.; Patterson, L. K. *J. Am. Chem. Soc.* **1975**, *97*, 89.

(27) Bunting, J. W.; Stefanidis, D. *J. Am. Chem. Soc.* **1988**, *110*, 4008.

This possibility was investigated by pumping BP solution through the flow device for 2 h, and then a solution containing the same BP concentration plus 0.04 M CTAB was injected. The absorbance at 272 nm was measured as a function of time (Figure 7). It was found that initially there was an increase in the absorption that reached its maximum at about 500 s. Thereafter it decreases. These results are different from the no-flow situation; i.e., the absorption of BP at 272 nm increases with the concentration of CTAB. They seem, however, to suggest that the BP molecules that had been adsorbed in the flow device were desorbed (extracted) by the CTAB micelles. This extraction leads to the increase in the absorbance at 272 nm. The absorbance started to decrease after all adsorbed BP molecules were extracted out.

### Conclusion

Several complexation reactions, e.g.,  $\beta$ -CD with phenolphthalein and aqueous micelles with BP and PTS were investigated. The complexation experiments were performed with and without flow conditions and the calculated binding constants and other model parameters were

compared between these two methods, as well as with the literature values (when available).

Under flow conditions, the calculated binding constants for the complexation reaction between PTS and CTAB and between  $\beta$ -CD and phenolphthalein are reproducible. In both cases (CTAB-PTS and  $\beta$ -CD-phenolphthalein complexes), the substrates were charged molecules.

The results obtained for BP, which has no charge, have relatively poor accuracy and reproducibility. Additionally, a completely unexpected absorption change as a function of CTAB concentration was observed under flow conditions. It is proposed that this effect is related to the adsorption of the BP molecules onto the flow device. This problem seems to occur mostly for hydrophobic molecules.

**Acknowledgment.** The authors are grateful to the National Institutes of Health, National Research Resources, Biomedical Technology Programs for financial support of this work. M.S. Baptista acknowledges CAPES for a fellowship.

LA9805894